Hund's rule, spin blockade, and the Aufbau principle in strongly confined semiconductor quantum dots

2000 Europhys. Lett. 50 243

(http://iopscience.iop.org/0295-5075/50/2/243)

EUROPHYSICS LETTERS 15 April 2000

Europhys. Lett., **50** (2), pp. 243–249 (2000)

Hund's rule, spin blockade, and the Aufbau principle in strongly confined semiconductor quantum dots

A. Franceschetti and A. Zunger

National Renewable Energy Laboratory - Golden, Colorado 80401, USA

(received 24 November 1999; accepted in final form 2 February 2000)

PACS. 73.20.Dx – Electron states in low-dimensional structures (superlattices, quantum well structures and multilayers).

Abstract. – The ground-state configuration of a system of N electrons or holes ($N = 1 \cdots 8$) in strongly confined InAs, InP, and Si quantum dots (diameter ~ 30 Å) is calculated using pseudopotential single-particle energies and wave functions as input to the many-body expansion of the total energy. The validity of generally accepted "rules of level occupation" (Hund's rule, Aufbau principle, and single spin-flip rule) is examined. We find that while Hund's rule is generally obeyed, deviations from the Aufbau principle are common when single-particle energy levels are separated by a few meV. We also find a few instances where the single spin-flip rule is violated, leading to "spin blockade" in linear conductance.

When a quantum dot is weakly coupled to an electron reservoir, either via a gate structure [1–4] or an STM tip [5,6], one can load, one by one, N electrons or holes into the dot by changing the gate voltage or the tip-substrate bias. The ability to successively load carriers into the dot enables one to study the "rules of level occupation" determining the sequence in which the energy levels of the dot are occupied. These rules are best illustrated by considering a dot with a pair of spatially degenerate single-particle energy levels e_{a1}, e_{a2} and a non-degenerate energy level e_b such that the single-particle energies obey $\varepsilon(e_{a1}) = \varepsilon(e_{a2}) < \varepsilon(e_b)$.

i) *Hund's rule*: Degenerate single-particle levels are occupied with a maximum number of unpaired electrons. For example, the transition from $N = 1$ to $N = 2$ electrons will prefer

$$e_{a1}^{\uparrow} \overset{\text{Hund}}{\longrightarrow} e_{a1}^{\uparrow}\, e_{a2}^{\uparrow} \tag{1a}$$

over

$$e_{a1}^{\uparrow} \overset{\text{Non-Hund}}{\longrightarrow} e_{a1}^{\uparrow}\, e_{a1}^{\downarrow}\,. \tag{1b}$$

This preference stems both from the gain of attractive exchange energy between the two parallel spin electrons in eq. (1a), and from the reduction of the repulsive electron-electron Coulomb energy via the placement of each electron in a separate spatial orbital ($e_{a1} \neq e_{a2}$).

ii) *The Aufbau principle*: Non-degenerate single-particle levels are occupied in order of increasing single-particle energy. For example, the $N = 2$ to $N = 3$ transition would prefer to

complete the occupation of the (e_{a1}, e_{a2}) shell before beginning to occupy the next (e_b) level:

$$e_{a1}^{\uparrow}\, e_{a2}^{\uparrow} \overset{\text{Aufbau}}{\longrightarrow} e_{a1}^{\uparrow}\, e_{a1}^{\downarrow}\, e_{a2}^{\uparrow} \tag{2a}$$

rather than

$$e_{a1}^{\uparrow}\, e_{a2}^{\uparrow} \overset{\text{Non-Aufbau}}{\longrightarrow} e_{a1}^{\uparrow}\, e_{a2}^{\uparrow}\, e_{b}^{\uparrow}\,. \tag{2b}$$

This preference stems from the saving of the $e_{a2} \to e_b$ promotion energy in process (2a).

iii) *Single spin-flip rule*: Each electron that is added to or removed from a dot changes the total number of unpaired electrons $N_{\rm u}$ by no more than one ($\Delta N_{\rm u} = \pm 1$). For example, the transition from $N = 3$ to $N = 4$ will prefer to reduce $N_{\rm u}$ from three to two ($\Delta N_{\rm u} = -1$):

$$e_{a1}^{\uparrow}\, e_{a2}^{\uparrow}\, e_{b}^{\uparrow} \overset{\Delta N_{\rm u}=-1}{\longrightarrow} e_{a1}^{\uparrow}\, e_{a1}^{\downarrow}\, e_{a2}^{\uparrow}\, e_{b}^{\uparrow} \tag{3a}$$

rather than to zero ($\Delta N_{\rm u} = -3$):

$$e_{a1}^{\uparrow}\, e_{a2}^{\uparrow}\, e_{b}^{\uparrow} \overset{\Delta N_{\rm u}=-3}{\longrightarrow} e_{a1}^{\uparrow}\, e_{a1}^{\downarrow}\, e_{a2}^{\uparrow}\, e_{a2}^{\downarrow}\,. \tag{3b}$$

In (3b) the addition of a single electron causes the spins of the previously present electrons to flip. Violation of the "single spin-flip rule" will lead to "spin blockade" effects, whereby transitions that violate this rule are missing in the linear conductance spectrum at zero temperature [7].

While early on only large (> 500 Å) quantum dots could be fabricated [8], it is now possible, via colloidal synthesis [9], to produce semiconductor nanocrystals whose dimensions are smaller than the bulk exciton radius ("strong confinement regime"). The electron and hole addition spectra in such dots are being studied experimentally using single-dot capacitance spectroscopy [4] or single-dot tunneling spectroscopy [5, 6]. Hund's rule was observed [3] to be obeyed in large (∼ 500 Å), electrostatically confined quantum dots, and was predicted [10] to be followed also in intermediate-size (∼ 200 Å) self-assembled quantum dots. It was not examined for strongly confined nanocrystals (∼ 30 Å). To our knowledge, the validity of the Aufbau principle was not discussed in detail. Finally, spin-blockade was predicted theoretically for simple 2D models of dots [7]. It was not studied for strongly confined quantum dots.

In this paper we study theoretically Hund's rule, the Aufbau principle, and the single spin-flip rule for semiconductor quantum dots (InAs, InP, and Si) in the strong-confinement regime. Unlike previous calculations based on a *continuum,* effective-mass description of the electronic structure [10–12], we use here an *atomistic* approach to calculate the single-particle energies and wave functions used as input to the many-body expansion of the total energy. We find that while Hund's rule is generally obeyed, deviations from the Aufbau principle are common when single-particle energy levels are separated by a few meV. For example, processes similar to the one described by eq. (2b) are the preferred transport channel in 30.3 Å diameter InAs dots for both electron and hole injection. We also find a few cases where the single spin-flip rule is not obeyed, and the transport channel (3b) is preferred over (3a). While the electron and hole occupation sequence is sensitive to the spacing of the single-particle energy levels, and therefore depends on the size and shape of the quantum dots, our results illustrate how single-particle effects can combine with interelectronic Coulomb and exchange effects to produce a particular occupation sequence.

In the screened Hartree-Fock approximation, the Hamiltonian of a charged quantum dot with a full valence band and a few electrons in the conduction band can be reduced to an

effective Hamiltonian involving only the conduction band electrons, provided that the electron-electron interaction is screened by the quantum dot dielectric constant:

$$\hat{H} = \sum_i \varepsilon_i \, c_i^\dagger \, c_i + \frac{1}{2} \sum_{ijkl} V(ij,kl) \, c_i^\dagger \, c_j^\dagger \, c_l \, c_k \,, \tag{4}$$

where $c_i^\dagger$ is the creation operator for an electron in the single-particle orbital i, c_i is the corresponding destruction operator, ε_i is the single-particle energy of the orbital i, and $V(ij,kl)$ are the screened Coulomb matrix elements:

$$V(ij,kl) = e^2 \sum_{\sigma,\sigma'} \int \int \frac{\psi_i^*(\boldsymbol{r},\sigma) \; \psi_j^*(\boldsymbol{r}',\sigma') \; \psi_k(\boldsymbol{r},\sigma) \; \psi_l(\boldsymbol{r}',\sigma')}{\epsilon(\boldsymbol{r},\boldsymbol{r}') \; |\boldsymbol{r}-\boldsymbol{r}'|} \; \mathrm{d}\boldsymbol{r} \, \mathrm{d}\boldsymbol{r}' \,, \tag{5}$$

calculated using the single-particle wave functions $\psi_i(\boldsymbol{r},\sigma)$. If we denote by $n_1, n_2, \cdots$ the occupation numbers of the conduction band energy levels (with $\sum_i n_i = N$) in a given configuration, the *diagonal* matrix elements of the Hamiltonian (4) are

$$E_N(n_1, n_2, \cdots) = \sum_i \varepsilon_i \, n_i + \sum_{i<j} (J_{i,j} - K_{i,j}) \, n_i \, n_j \,, \tag{6}$$

where $J_{i,j} \equiv V(ij,ij)$ and $K_{i,j} \equiv V(ij,ji)$ are the diagonal Coulomb and exchange energies, respectively [13]. The *off-diagonal* matrix elements of the Hamiltonian (4) introduce coupling between different configurations.

The single-particle energies ε_i and wave functions $\psi_i(\boldsymbol{r},\sigma)$ are obtained here from the solution of the Schrödinger equation

$$\left[-\frac{\hbar^2}{2m} \nabla^2 + V_{\mathrm{ps}}(\boldsymbol{r}) + \hat{V}_{\mathrm{nl}} \right] \psi_i(\boldsymbol{r},\sigma) = \varepsilon_i \, \psi_i(\boldsymbol{r},\sigma) \,, \tag{7}$$

where m is the bare electron mass, $V_{\mathrm{ps}}(\boldsymbol{r})$ is the total pseudopotential of the system (dot + ligands that passivate the surface dangling bonds), and $\hat{V}_{\mathrm{nl}}$ is a short-range operator that accounts for the non-local part of the potential and for spin-orbit coupling. The pseudopotential $V_{\mathrm{ps}}(\boldsymbol{r})$ is calculated from the superposition of local atomic pseudopotentials, which are fitted to reproduce the measured bulk transition energies, deformation potentials, and effective masses, as well as the bulk single-particle wave functions calculated using density-functional theory in the local-density approximation [14]. The pseudopotentials used here are from ref. [15] (InAs), ref. [16] (InP), and ref. [17] (Si). The solution of eq. (7) is performed by expanding the wave functions $\psi_i(\boldsymbol{r},\sigma)$ in a plane-wave basis set, and calculating the near-edge states using the folded spectrum method [17]. The screened Coulomb integrals $V(ij,kl)$ of eq. (5) are calculated using the atomistic pseudopotential wave functions obtained from eq. (7). We use a phenomenological model [18] for the microscopic dielectric function $\epsilon(\boldsymbol{r},\boldsymbol{r}')$, which depends both on the interparticle separation $(\boldsymbol{r}-\boldsymbol{r}')$ and on the quantum dot radius R. For $\boldsymbol{r} \to \boldsymbol{r}'$ the dielectric function tends to 1 (regardless of the dot radius R), so that the short-range interaction is unscreened. For $|\boldsymbol{r}-\boldsymbol{r}'| \gg$ (interatomic bond length) the screening function approaches the quantum dot macroscopic dielectric constant, which depends on the dot radius R [18].

The many-particle Hamiltonian of eq. (4) is diagonalized in a *single-configuration* basis set. In this approach, we construct a set of N-particle Slater determinants $|n_1, n_2, \cdots\rangle$, such that $\sum_i n_i = N$. We then retain the Hamiltonian matrix elements between Slater determinants that are degenerate at the single-particle level, as a consequence of spatial degeneracy or spin

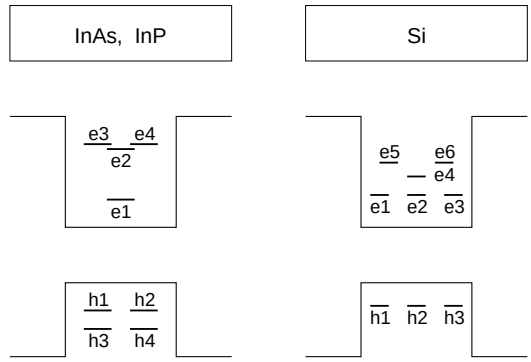

Fig. 1 – Schematic diagram of the near band-edge single-particle energy levels of InAs, InP, and Si spherical quantum dots. The valence band levels are denoted as h_1, h_2, etc. in order of decreasing energy starting from the valence band maximum, while the conduction band levels are denoted as e_1, e_2, etc. in order of increasing energy starting from the conduction band minimum.

degeneracy of the single-particle orbitals. Finally, the ground-state configuration for a given number N of electrons (or holes) is obtained by scanning different single configurations and diagonalizing the many-particle Hamiltonian (4) in search of the configuration with the lowest energy.

Our approximations are: i) The single-particle energies and wave functions are obtained by solving eq. (7) for a fixed, non–self-consistently screened potential. This approximation was examined in the case of an exciton [19] by comparing the electron-hole Coulomb integral obtained using non–self-consistent wave functions with the result of a self-consistent calculation. The difference was less than 5%. ii) The single-configuration approach used to diagonalize the many-particle Hamiltonian of eq. (4) neglects correlation effects due to configuration mixing. These effects were examined in ref. [18], and found to be small in strongly confined quantum dots. iii) Surface-polarization effects, which exist if the dielectric constant of the dot is different from that of the surrounding material, are neglected. This appoximation is valid when $\epsilon_{\rm out} \sim \epsilon_{\rm in}$.

We consider here InAs, InP and Si spherical quantum dots having the T_d point-group symmetry. The surface dangling bonds are fully passivated. The single-particle energy levels calculated using pseudopotentials [15–17] have the general pattern shown in fig. 1. Each energy level in fig. 1 is doubly degenerate because of time reversal symmetry, and can be occupied by two particles (either electrons or holes). In the case of InAs and InP dots the two degenerate single-particle levels at the top of the valence band (h_1 and h_2) originate from the bulk Γ_{8v} states, and have an s-like envelope function. The next two degenerate hole levels (h_3 and h_4) are also Γ_{8v}-derived, but have p-like envelope functions. The electron level at the bottom of the conduction band (e_1) originates from the bulk Γ_{6c} state and has an s-like envelope function. In InAs dots the next three electron levels (e_2, e_3, and e_4) derive from the bulk Γ_{6c} state and have a p-like envelope function [15] (e_2 is split from e_3 and e_4 because of spin-orbit coupling, as well as numerical approximations in the non-local pseudopotential); in InP dots e_2, e_3, and e_4 originate from the L_{6c} bulk states and have s-like envelope function [16]. In the case of Si dots (where spin-orbit coupling is not included, and therefore only electron states are considered) the six levels at the bottom of the conduction band originate from the bulk conduction band minima located near the X points of the Brillouin zone and have an s-like envelope function [20].

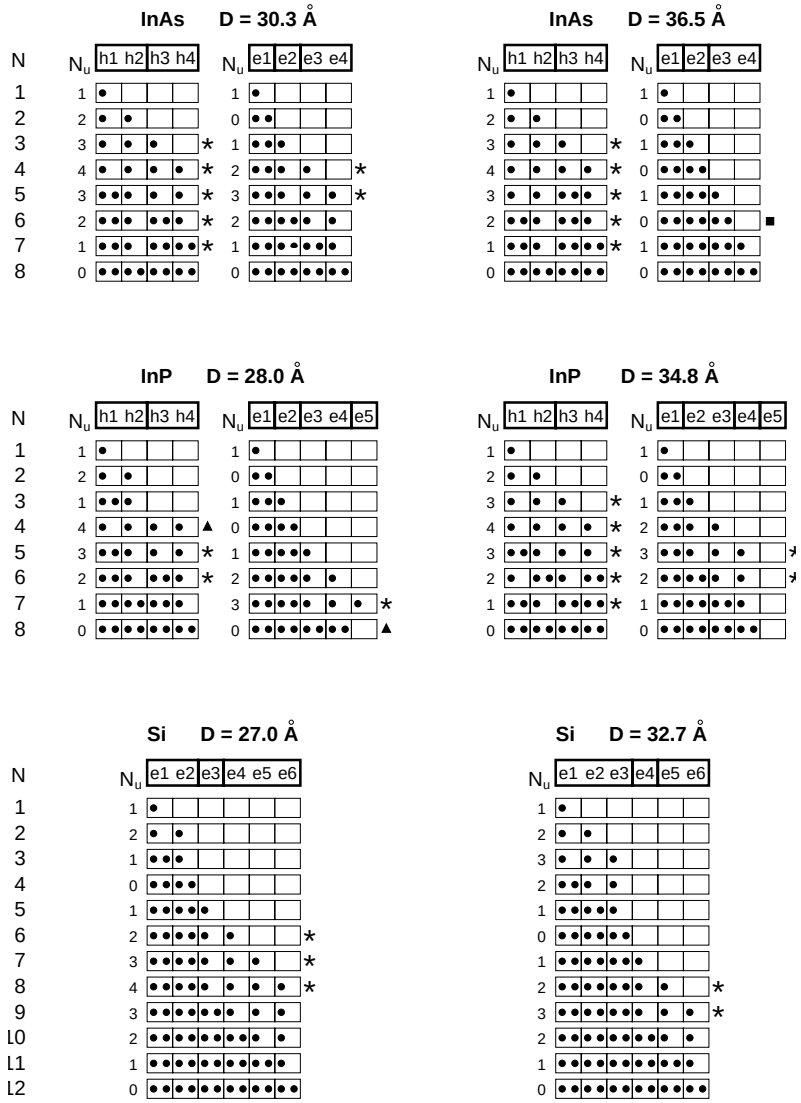

Fig. 2 – Lowest-energy configurations of a system of N electrons (or N holes) in selected InAs, InP and Si quantum dots. The header of each figure shows the single-particle energy levels grouped according to their degeneracy. The number of unpaired electrons or holes in each configuration N_{u} is shown on the left-hand side of each column. A solid square to the right of a configuration marks violation of Hund's rule, an asterisk denotes violation of the Aufbau principle, while a triangle indicates violation of the single spin-flip rule.

Figure 2 shows the electron and hole occupation sequences of InAs, InP, and Si quantum dots that give the lowest total energies in our single-configuration approach.

i) *Hund's rule*: We find that when two or more energy levels are degenerate, double occupation of one of them is generally avoided so as to maximize the exchange energy and minimize the interelectronic Coulomb energy. For example, in the case of InAs and InP dots, the two energy levels at the top of the valence band (h_1 and h_2) are degenerate, so if two

holes are present in the quantum dot each of these two levels is occupied by one hole. In the diagonal approximation of eq. (6), the energy difference between the Hund configuration $(h_1^1\,h_2^1)$ and the non-Hund configuration $(h_1^2\,h_2^0)$ is $\Delta E_2 = E_2(h_1^1\,h_2^1) - E_2(h_1^2\,h_2^0) = J_{h1,h2} - J_{h1,h1} - K_{h1,h2}$. For a 30.3 Å diameter InAs dot we find $\Delta E_2 = 166 - 172 - 6 = -12\,\mathrm{meV}$; for a 36.5 Å diameter InAs dot $\Delta E_2 = 137 - 141 - 4 = -8\,\mathrm{meV}$. Thus, only about half of the stabilization of the Hund configuration comes from interelectronic exchange. The other half comes from the reduction in the Coulomb repulsion achieved by placing the two holes in different spatial orbitals. We find only one case where Hund's rule is violated: When six electrons are loaded into a 36.5 Å diameter quantum dot, two of them occupy the e_3 level, while the e_4 level (degenerate with e_3) is empty. This is due to the fact that the coupling between the configurations $(e_1^2\,e_2^2\,e_3^2)$ and $(e_1^2\,e_2^2\,e_4^2)$, which are degenerate at the single-particle level, is sufficiently strong to overcome the exchange and Coulomb energies gained by placing the electrons in the configuration $(e_1^2\,e_2^2\,e_3^1\,e_4^1)$.

ii) *The Aufbau principle*: We find several instances where the Aufbau principle is not obeyed. For example, in InAs dots for $N_{\mathrm{holes}} = 3 \cdots 7$ the hole levels h_3 and h_4 are occupied before the levels h_1 and h_2 are filled. For $N = 3$, the diagonal-energy difference between the non-Aufbau configuration $(h_1^1\,h_2^1\,h_3^1)$ and the Aufbau configuration $(h_1^2\,h_2^1)$ is $\Delta E_3 = (\varepsilon_{h2} - \varepsilon_{h3}) + (J_{h1,h3} + J_{h2,h3} - J_{h1,h1} - J_{h1,h2}) - (K_{h1,h2} + K_{h2,h3})$. In the case of the 36.5Å diameter InAs dot we find $\Delta E_3 = 23 - 22 - 14 = -13\,\mathrm{meV}$. Another example of violation of the Aufbau principle is the 27.0Å diameter Si dot, where for $N_{\mathrm{electron}} = 6 \cdots 8$ the shell consisting of the electron levels e_4, e_5, and e_6 is occupied before the level e_3 is filled. For $N = 6$, the energy difference between the non-Aufbau configuration $(e_1^2\,e_2^2\,e_3^1\,e_4^1)$ and the Aufbau configuration $(e_1^2\,e_2^2\,e_3^2)$ is $\Delta E_6 = (\varepsilon_{e4} - \varepsilon_{e3}) + (2J_{e1,e4} + 2J_{e2,e4} - 2J_{e1,e3} - 2J_{e2,e3} + J_{e3,e4} - J_{e3,e3}) - (K_{e1,e4} + K_{e2,e4} + K_{e3,e4} - K_{e1,e3} - K_{e2,e3}) = 4 - 6 - 3 = -5\,\mathrm{meV}$. We see that the Aufbau principle can be violated due to a delicate balance between promotion energies, Coulomb repulsion, and exchange interaction.

iii) *"Spin blockade"*: The number of unpaired particles (electrons or holes) N_{u} usually changes by one when a particle is added to the quantum dot: $\Delta N_{\mathrm{u}} = \pm 1$. This is the case when upon addition of the N-th particle to the dot the configuration of the $N-1$ particles already residing in the dot remains unchanged. We find a few exceptions to this rule. In the 28.0 Å diameter InP dot the addition of the 4-th hole to the dot causes the number of unpaired holes to change from $N_{\mathrm{u}} = 1$ to $N_{\mathrm{u}} = 4$:

$$h_1^2\,h_2^1 \rightarrow h_1^1\,h_2^1\,h_3^1\,h_4^1\,. \tag{8}$$

Similarly, when the 8-th electron is added to the 28.0 Å diameter InP dot the number of unpaired electrons changes from $N_{\mathrm{u}} = 3$ to $N_{\mathrm{u}} = 0$:

$$e_1^2\,e_2^2\,e_3^1\,e_4^1\,e_5^1 \rightarrow e_1^2\,e_2^2\,e_3^2\,e_4^2\,. \tag{9}$$

The energy difference between the configuration $(e_1^2\,e_2^2\,e_3^2\,e_4^2)$ and, for example, the configuration $(e_1^2\,e_2^2\,e_3^2\,e_4^1\,e_5^1)$ is $-2\,\mathrm{meV}$, which includes a $-4\,\mathrm{meV}$ single-particle energy difference, a $-8\,\mathrm{meV}$ Coulomb energy difference and a $+10\,\mathrm{meV}$ exchange energy difference.

In conclusion, using a many-particle approach based on atomistic pseudopotential wave functions, we have calculated the lowest-energy configuration of a system of N electrons or N holes in small semiconductor quantum dots. We have discussed the validity of the "rules of level occupation", such as Hund's rule, the Aufbau principle, and the single spin-flip rule. While Hund's rule is generally obeyed, we find several deviations from the Aufbau principle, and a few cases where the single spin-flip rule is violated, leading to "spin blockade".

* * *

This work was supported by the U.S. DOE, OER-SC, Division of Materials Science, under Grant No. DE-AC36-98-GO10337.

REFERENCES

[1] Mceuen P. L., Foxman E. B., Meirav U., Kastner M. A., Meir Y., Wingreen N.S. and Wind S. J., *Phys. Rev. Lett.*, **66** (1991) 1926.
[2] Weis J., Haug R. J., von Klitzing K. and Ploog K., *Phys. Rev. Lett.*, **71** (1993) 4019.
[3] Tarucha S., Austing D. G., Honda T., van der Hage R. J. and Kouwenhoven L. P., *Phys. Rev. Lett.*, **77** (1996) 3613.
[4] Klein D. L., Roth R., Lim A. K. L., Alivisatos A. P. and Mceuen P. L., *Nature*, **389** (1997) 1.
[5] Banin U., Cao Y., Katz D. and Millo O., *Nature*, **400** (1999) 542.
[6] Alperson B., Rubinstein I., Hodes G., Porath D. and Millo O., *Appl. Phys. Lett.*, **75** (1999) 1751.
[7] Weinmann D., Häusler W. and Kramer B., *Phys. Rev. Lett.*, **74** (1995) 984.
[8] Reed M. A., Randall J. N., Aggarwal R. J., Matyi R. J., Moore T. M. and Wetsel A. E., *Phys. Rev. Lett.*, **60** (1988) 535.
[9] Murray C. B., Norris D. J. and Bawendi M. G., *J. Am. Chem. Soc.*, **115** (1993) 8706.
[10] Fonseca L. R. C., Jimenez J. L., Leburton J. P. and Martin R. M., *Phys. Rev. B*, **57** (1998) 4017.
[11] Wojs A. and Hawrylak P., *Phys. Rev. B*, **53** (1996) 10841.
[12] Rontani M., Rossi F., Manghi F. and Molinari E., *Appl. Phys. Lett.*, **72** (1998) 957.
[13] Strictly speaking, the diagonal energies $E_N(n_1, n_2, \cdots)$ may not be well defined for degenerate configurations, as they depend on the particular linear combination of degenerate single-particle states selected by the numerical solution of the Schrödinger equation. However, this dependence is usually weak, and the diagonal energies can still be utilized for quantitative estimates.
[14] Wang L. W. and Zunger A., *Phys. Rev. B*, **51** (1995) 17398.
[15] Williamson A. and Zunger A., *Phys. Rev. B*, **61** (2000) 1978.
[16] Fu H. and Zunger A., *Phys. Rev. B*, **55** (1997) 1642.
[17] Wang L. W. and Zunger A., *J. Chem. Phys.*, **100** (1994) 2394; *J. Phys. Chem.*, **98** (1994) 2158.
[18] Franceschetti A., Fu H., Wang L. W. and Zunger A., *Phys. Rev. B*, **60** (1999) 1819.
[19] Franceschetti A., and Zunger A., *Phys. Rev. Lett.*, **78** (1997) 915.
[20] Reboredo F., Franceschetti A. and Zunger A., *Appl. Phys. Lett.*, **75** (1999) 2972.